DØnote 5263-Conf

# Measurement of the Lambda-b Lifetime Using Semileptonic Decay


The DØ Collaboration
*URL: http://www-d0.fnal.gov*


(Dated: October 28, 2006)



We report a preliminary measurement of the $\Lambda_b^0$ lifetime using approximately 1.3 fb$^{-1}$ of data collected by the DØ detector in Run 2a. The $\Lambda_b^0$ was reconstructed using the decay $\Lambda_b^0 \rightarrow \Lambda_c^+ \mu^- \overline{\nu}_\mu X$. A signal of 4437 $\pm$ 329 events was obtained, and the lifetime was measured to be $\tau(\Lambda_b^0) = 1.28\ ^{+0.12}_{-0.11}$ (stat) $\pm$ 0.09 (syst) ps.


*Preliminary Results for DPF Conference*

## I. INTRODUCTION

Lifetimes of $B$ hadrons provide an important test of different models describing quark interaction within bound states. The experimental measurement of the lifetimes has thus far given reasonable agreement with the theoretical values, but a further improvement in precision of both the theoretical predictions and experimental results is essential for the development of the non-perturbative QCD.

This paper presents the measurement of the $\Lambda_b^0$ lifetime using semileptonic decay $\Lambda_b^0 \to \mu\bar{\nu}\Lambda_c^+ X$, where $X$ is any other particle. Charge conjugates are implied throughout this paper. The $\Lambda_c^+$ was selected in the decay $\Lambda_c^+ \to K_S^0 p^+$ using data from approximately 1.3 fb$^{-1}$ integrated luminosity, collected by the DØ detector throughout the whole of Run 2a.

## II. EVENT SELECTION

A trigger selection was first applied to select those events which satisfy only triggers which do not bias the lifetime distribution. The selection of events was then performed using criteria which are not expected to produce a lifetime bias, as checked by Monte Carlo simulations. For each event the primary vertex was determined using the method described in [1] and the charged particles were clustered into jets using the DURHAM clustering algorithm [2]. Muons were selected using the standard DØ tools [3] and were then also required to have at least two track segments in the muon chambers associated to a central track and a value of $p_T$ of at least 2.0 GeV/$c$. The products from the decay of $\Lambda_c^+$ were then searched for among tracks belonging to the same jet as an identified muon.

The tracks of two oppositely charged particles were required to form a secondary vertex with a $\chi^2$ of less than 25 and a distance $d_{V^0}$ from the primary vertex of at least $4\sigma(d_{V^0})$. The two tracks were assumed to be $\pi^+\pi^-$ and their invariant mass was calculated. The pairs with invariant mass within the range 0.4800 GeV/$c^2$ – 0.5075 GeV/$c^2$ were accepted as $K_S^0$ candidates. These limits both correspond to approximately $1.8\sigma$ away from the center of the mass peak, where $\sigma$ is the fitted width of the $K_S^0$ mass peak. Either of these oppositely charged tracks was assumed to be a proton, and if the resulting invariant mass lay between 1.109 and 1.120 GeV/$c^2$, the $K_S^0$ candidate was rejected since this mass range is consistent with the decay $\Lambda^0 \to p\pi$. This veto reduces the sample size by approximately 4%.

For each reconstructed $K_S^0$ candidate, the remaining tracks in the jet were searched for a proton candidate. Each track with $p_T > 1.0$ GeV/$c$ and at least 2 hits in the silicon detector was combined with the $K_S^0$ to form a $\Lambda_c^+$ candidate. Their common vertex was required to have a value of $\chi^2$ less than 9. The $\Lambda_c^+$ candidate was combined with the muon to make a $\Lambda_b^0$ candidate and its invariant mass was required to be greater than 3.4 GeV/$c^2$ and less than 5.4 GeV/$c^2$. A common vertex of $\Lambda_c^+$ and muon was required to have the $\chi^2$ of vertex fit less than 9. The transverse distance $d_T^{bc}$ between the $\Lambda_b^0$ and $\Lambda_c^+$ vertices was calculated. It was assigned a positive sign if the $\Lambda_b^0$ vertex is closer to the primary vertex, and a negative sign otherwise. The $\Lambda_b^0$ candidate was required to have $-3 < d_T^{bc}/\sigma(d_T^{bc}) < 3.3$, where $\sigma(d_T^{bc})$ is the precision of $d_T^{bc}$. The upper limit on the distance between $\Lambda_b^0$ and $\Lambda_c^+$ vertices helps to reduce the background significantly, since the lifetime of $\Lambda_c^+$ is known to be very small [4]. The transverse momentum of the muon with respect to the direction of the $\Lambda_c^+$ candidate was required to be greater than 0.35 GeV/$c$. A cone of $\sqrt{(\Delta\phi)^2 + (\Delta\eta)^2} < 0.5$ was defined around the momentum of the $\Lambda_c^+\mu$ system, where $\Delta\phi$ and $\Delta\eta$ are the pseudo-rapidity and azimuthal angle from the direction of the $\Lambda_c^+\mu$ system. The momenta of all tracks within this cone - excluding the muon, pions from $K_S^0$ decay and the proton from $\Lambda_c^+$ decay - were then summed, and the momentum of the $\Lambda_b^0$ candidate added. The isolation was defined as the fraction of the total momentum within the cone carried by the $\Lambda_b^0$ candidate. To reduce background this was required to be greater than 0.5.

To further reduce background a likelihood ratio method was used. A set of discriminating variables $x_1, ..., x_n$ was selected. For each variable a pair of probability density functions was defined, one for the signal events, $f^s$, and another for the background events, $f^b$. A combined variable $y$ was defined as follows:

$$y = \prod_{i=1}^{n} y_i; \quad y_i = \frac{f_i^b(x_i)}{f_i^s(x_i)} \tag{1}$$

The following discriminating variables were used:

- Isolation, defined as above;
- $p_T(K_S^0)$;
- $p_T$ of proton;
- $p_T(\Lambda_c^+)$;

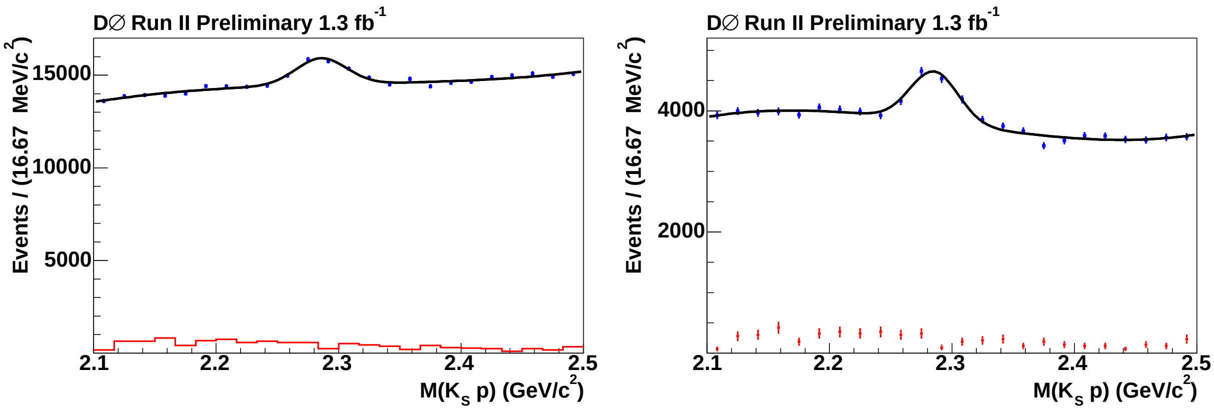


FIG. 1: LEFT: the $K^0_S p$ invariant mass for the selected $\Lambda^0_b$ candidates. The lower histogram shows the shape of, and approximate level of the expected contribution of decay $B_d \to D\mu\nu(D \to K^0_S\pi)$ when a pion is assigned the mass of proton. RIGHT: The mass plot for events with the visible proper decay length greater than 0.02 cm. The lower histogram shows the shape of reflection from $B_d$ decay.

- $M(\mu + \Lambda^+_c)$

The probability density functions both for a signal and background were obtained directly in data using the decays $B^0_d \to D^-\mu^+X(D \to K^0_S\pi)$ and $B^0_s \to D^-_s\mu^+X(D_s \to K^0_S K)$ which have a kinematics similar to the studied $\Lambda^0_b$ decay.

Figure 1 shows the invariant mass of the $\Lambda^+_c$ candidates with all selections applied. The fit to this distributions was performed with a signal Gaussian and a fourth order polynomial background. The fitted $\Lambda^0_b$ signal contains 4437 $\pm$ 329 events at a central mass of 2285.80 $\pm$ 1.7 MeV/$c^2$. The width of the mass peak is 20.56 $\pm$ 1.74 MeV/$c^2$. The shape and approximate level of the expected contribution of decay $B_d \to D\mu\nu(D \to K^0_S\pi)$ when a pion is assigned the mass of proton is also shown in Fig. 1. It can be seen that the reflected events have a wide distribution with no excess close to the $\Lambda^+_c$ mass. Also shown in Fig. 1 is the plot of $M(K^0_S p)$ when the visible proper decay length $\lambda$ is required to be greater than 0.02 cm, to illustrate the increased significance of the signal for larger lifetimes.

## III. VISIBLE PROPER DECAY LENGTH AND K-FACTOR

To perform the lifetime fit the transverse decay length, $L_{xy}$ was measured for each event. The $L_{xy}$ was defined as the projection of the vector $\vec{X}$ from the primary to the $\Lambda^0_b$ vertex on the transverse momentum of the $(\Lambda^+_c\mu)$ system:

$$L_{xy} = \frac{\vec{X} \cdot \vec{p_T}(\Lambda^+_c\mu)}{|p_T(\Lambda^+_c\mu)|}. \tag{2}$$

In terms of the lifetime of a $\Lambda^0_b$, $\tau(\Lambda^0_b)$, the transverse decay length is given by

$$L_{xy} = \frac{c\tau(\Lambda^0_b)p_T(\Lambda^0_b)}{m}. \tag{3}$$

In semileptonic decays $p_T(\Lambda^0_b)$ cannot be measured, so instead $p_T(\Lambda^+_c\mu)$ was used. For each event the visible proper decay length(VPDL), $\lambda$, is calculated, using the following relation:

$$\lambda = L_{xy}\frac{m}{p_T(\Lambda^+_c\mu)} = \frac{c\tau(\Lambda^0_b)}{K}. \tag{4}$$

The $K$ factor was introduced into the fitting procedure to correct for the difference in transverse momentum of $(\Lambda^+_c\mu)$ and $\Lambda^0_b$:

$$K = \frac{p_T(\Lambda^+_c\mu)}{p_T(\Lambda^0_b)}. \tag{5}$$

| | $\Lambda_b^0 \to \Lambda_c^+ \mu\nu_\mu$ | $\Lambda_b^0 \to \Sigma_c \pi \mu\nu_\mu$ | $\Lambda_b^0 \to \Lambda_c^+ D_s^{(*)}$ |
|---|---|---|---|
| Relative Branching Fraction | 1 | 1.6915 | 0.6567 |
| $\langle K \rangle$ | 0.8933 | 0.8010 | 0.7940 |
| Relative Efficiency | 1 | 0.342 | 0.193 |
| $f_K$ | 0.5861 | 0.3395 | 0.0744 |

TABLE I: The average value of $K$ factor, reconstruction efficiency and relative fraction of different processes in the selected sample.

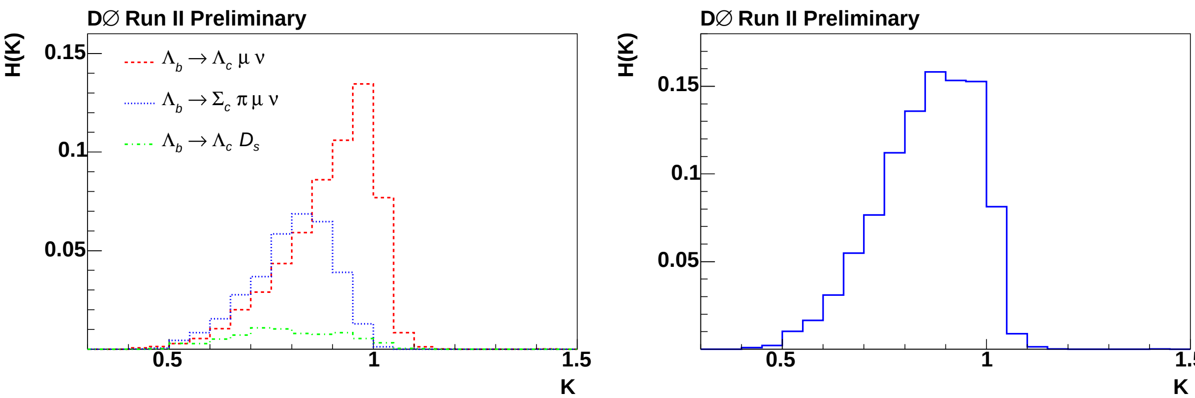


FIG. 2: LEFT: $K$-factor distributions for the different processes. RIGHT: $K$-factor distribution for the included processes combined, according to their relative predicted fractions.

The probability distribution for the $K$ factor was determined using Monte Carlo events. The generated sample included decays $\Lambda_b^0 \to \Lambda_c^+ \mu\nu$ and $\Lambda_b^0 \to \Sigma_c \pi\mu\nu$, where the $\Sigma_c$ decays strongly to $\Lambda_c^+\pi$. The indirect decay has a softer $p_T(\Lambda_c^+\mu)$, and hence a different $K$ factor distribution. The decay $\Lambda_b^0 \to \Lambda_c^+ D_s^{(*)-}$ with the semileptonic decay of $D_s^{(*)-}$ can also be reconstructed, although with a lower efficiency, and also have a different $K$ factor distribution. We generated a sample with equal fractions of the decays $\Lambda_b^0 \to \Lambda_c^+ D_s^-$ and $\Lambda_b^0 \to \Lambda_c^+ D_s^*$.

The $K$ factor distribution for each of the three contributions is shown in Figure 2, where they are shown in the relative fractions that are estimated for the sample. The final state of $\Lambda_c^+ l^- \bar{\nu}_l$ has been observed to contribute a fraction of $0.47^{+0.12}_{-0.10}$ of the total semileptonic $\Lambda_b^0$ decays [4]. We use this estimate in our analysis. The branching fraction for $\Lambda_b^0 \to \Lambda_c^+ D_s^{(*)-}$ is not known. The default value set in our simulation was varied in a wide range to estimate the impact of this uncertainty on our measurement. The efficiency of reconstruction of all processes was estimated in the simulation and is given in Table I.

It is also possible that the decay of $\Lambda_b^0 \to \Lambda_c^+ \tau^- \bar{\nu}_\tau$ is reconstructed. However the fraction of this decay is suppressed due to the branching fraction of $\tau \to \mu\bar{\nu}_\mu\nu_\tau$ of approximately 18%. Also the reconstruction efficiency is lower, so this decay gives only a few percent contribution and is taken into account in the systematics.

## IV. $c\bar{c}$ BACKGROUND

$\Lambda_c^+$ baryons can also be created in prompt $c\bar{c}$ production, along with muons that are produced from the decay of another charm hadron. These will be reconstructed as $\Lambda_b^0$ candidates but will have a pseudo decay vertex formed by the crossing of muon and $\Lambda_c^+$ tracks very close to the primary interaction point. These events are expected to give a significant fraction of the reconstructed signal, so this contribution must be taken into account in the fit. Monte Carlo simulation for this process was generated and the visible proper decay length distribution for the reconstructed events was fitted with a double Gaussian, as shown in Fig. 3. This shape was used to model the $c\bar{c}$ contribution in the lifetime fit. The parameters later varied in accordance with the given uncertainties to estimate the systematic effect on the fitted $\Lambda_b^0$ lifetime.

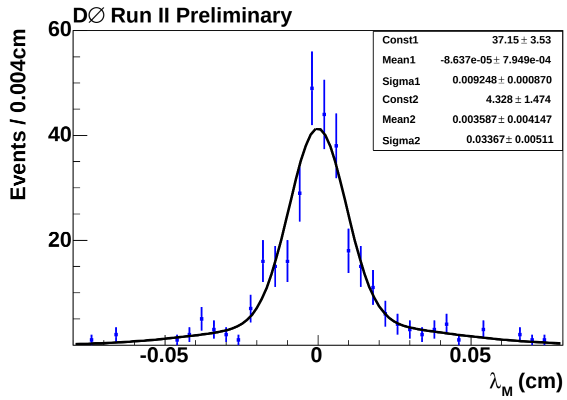


FIG. 3: Reconstructed visible proper decay length distribution for Monte Carlo $c\bar{c}$ events passing the selections used in this analysis

## V. LIFETIME FIT

Usually when performing a lifetime fit an unbinned maximum likelihood method is used, however the large backgrounds in this sample cause problems for this technique. Therefore, to determine the $\Lambda_b^0$ lifetime, the selected sample was split into a number of bins with the visible proper decay length $\lambda$ within different ranges. The mass distribution in each of these bins was fitted with a signal Gaussian and a fourth degree polynomial background, as shown in Figure 4. The range of $\lambda$ and the number of signal events fitted in each bin are shown in Table II. The expected number of signal events in each bin for a set of parameters can be calculated and the lifetime obtained by the minimization of $\chi^2$:

$$\chi^2 = \sum_{i}^{N_{bins}} \frac{(n_i - N_{tot} \cdot P_i)^2}{\sigma_i^2}, \tag{6}$$

where $N_{tot}$ is the total number of signal events, $N_{bins}$ is the number of VPDL bins, and $P_i$ is the probability for the measured visible proper decay length $\lambda_M$ to be within bin $i$. Hence $P_i$ is given by

$$P_i = \int_i p(\lambda_M) d\lambda_M, \tag{7}$$

where $p(\lambda_M)$ is the probability density function for the measured visible proper decay length $\lambda_M$. The integration is done over the bin range. As well as the signal there is also a contribution from $c\bar{c}$ background to the signal peak so $p(\lambda_M)$ is given by:

$$p(\lambda_M) = (1 - f_{c\bar{c}}) p_{sig}(\lambda_M) + f_{c\bar{c}} G_{c\bar{c}}(\lambda_M - \lambda), \tag{8}$$

where $p_{sig}(\lambda_M)$ is the measured VPDL distribution for the signal events, and $G_{c\bar{c}}(\lambda_M - \lambda)$ is the double Gaussian distribution used to model the $c\bar{c}$ background, as shown in Figure 3.

The probability density function for the signal events is given by:

$$p_{sig}(\lambda_M) = \int dK H(K) \left[ \frac{K}{c\tau_{\Lambda_b^0}} e^{-K\lambda / c\tau_{\Lambda_b^0}} \otimes R(\lambda_M - \lambda, s) \right] \tag{9}$$

The exponential decay function is convoluted with the resolution function to obtain the observed distribution for each value of $K$-factor, and then integrated over the $K$-factor distribution using the $K$ factor probability density function $H(K)$. The resolution function is given by:

$$R(\lambda_M - \lambda, s) = \int p(\sigma) G(\lambda_M - \lambda, \sigma, s) d\sigma, \tag{10}$$

where $p(\sigma)$ is the probability density function for the VPDL uncertainty of the signal events, and $G$ is a Gaussian function:

$$G(\lambda_M - \lambda, \sigma, s) = \frac{1}{\sqrt{2\pi}\sigma s} e^{\frac{-(\lambda_M - \lambda)^2}{2(s\sigma)^2}}. \tag{11}$$

| VPDL range(cm) | Number of signal events |
|---|---|
| $[-0.06, -0.04]$ | $62 \pm 48$ |
| $[-0.04, -0.02]$ | $66 \pm 69$ |
| $[-0.02, 0.00]$ | $587 \pm 156$ |
| $[0.00, 0.02]$ | $1172 \pm 173$ |
| $[0.02, 0.04]$ | $999 \pm 99$ |
| $[0.04, 0.06]$ | $540 \pm 69$ |
| $[0.06, 0.08]$ | $299 \pm 54$ |
| $[0.08, 0.10]$ | $225 \pm 44$ |
| $[0.10, 0.20]$ | $454 \pm 64$ |
| $[0.20, 0.30]$ | $47 \pm 34$ |

TABLE II: Fitted Signal Yield in VPDL bins

Here a resolution scale factor $s$ was included, to account for misestimate of the VPDL precision. The distribution of the VPDL uncertainty for signal events was determined using a subsample of events with an additional cut $\lambda > 200$ $\mu$m. To do this, the signal and background bands were defined in this subsample according to the mass of $K^0_S p$ system. The $(K^0_S p)$ mass distribution of these events is shown in Fig. 1 (right plot). All events with $2244.68 < M(K^0_S p) < 2326.92$ MeV/$c^2$ were included in the signal band, and all events with $2183.88 < M(K^0_S p) < 2225$ MeV/$c^2$ and $2346.6 < M(K^0_S p) < 2387.72$ MeV/$c^2$ were included in the background band. The VPDL uncertainty distribution was obtained by subtracting the distribution for the background band from the distribution for the signal band.

The free parameters of the fit were $N_{tot}$, $\tau_{\Lambda^0_b}$ and $f_{c\bar{c}}$. A separate study was performed to measure in data the resolution scale factor for vertices constructed by crossing $K^0_S$ and charged tracks and the scale factor $s = 1.19 \pm 0.06$ was found. It was fixed to this value in the lifetime fit and varied later in a wide range to estimate an associated systematic uncertainty. The lifetime fit gives $c\tau(\Lambda^0_b) = 384.3^{+35.4}_{-32.8}$ (stat) $\mu$m and the fraction of $c\bar{c}$ events $f_{c\bar{c}} = 0.159^{+0.068}_{-0.074}$ (stat). Figure 5 shows the distribution of the number of $\Lambda^+_c\mu$ events versus the VPDL with the result of the lifetime fit superimposed. The lifetime model agrees well with data with $\chi^2/NDF = 0.79$. A dashed line shows separately the $c\bar{c}$ contribution. The fitted value of the $c\bar{c}$ contribution is consistent with that found in other DØ analyses [5].

## VI. SYSTEMATIC UNCERTAINTIES

The method used to fit the mass distribution in each of the VPDL bins is the most significant source of systematic uncertainty. To estimate its magnitude, the model for the background description was varied, as well as the binning of the mass plots. A linear background model was used and each VPDL bin refitted within the mass interval between 2.17 and 2.40 GeV/$c^2$. Another test involved shifting the bins of the histograms by half of a bin width. Also the fits were performed with bins of half the width, and with the highest and lowest bins removed. The lifetime fit was performed again for each test. The largest deviation of the fitted value of $c\tau$ was 20 $\mu m$, so we give this as the systematic uncertainty due to the mass fitting procedure.

The width of the two Gaussians and the fraction of the wide Gaussian used in the fitting of the $c\bar{c}$ distributions were varied by their uncertainties and the variation of the fitted lifetime observed. The largest shift in the fitted lifetime was 2.4 $\mu$m. The width of the $c\bar{c}$ distribution is mainly due to the distribution of the fake vertices, but the resolution may also contribute. Since the resolution is underestimated in the data, the widths of both Gaussians were increased by 20%, and the shift of approximately 1 $\mu m$ due to this was added in quadrature with the above error to give a total systematic uncertainty of 2.6 $\mu m$. Since the resolution will be less important in the $c\bar{c}$ than in the signal this should be a conservative estimate.

The value of the scale factor was varied by $\pm 20\%$, and shifts of approximately $\mp$ 10 $\mu m$ were observed in the fitted lifetime, so this value was also included in the systematics.

To estimate the systematic uncertainty due to unknown branching fractions of different processes used to generate the $K$-factor distribution, they were varied over a wide range. The fraction of $\Sigma_c \pi\mu\nu_\mu$ and $\Lambda^+_c D^{(*)-}_s$ decays relative to $\Lambda^+_c \mu\nu_\mu$ was increased by 50%. This is a wide variation compared to the errors on the $\Sigma_c\pi\mu\nu_\mu$ branching fraction, which accounts for small contributions from decays to $\Lambda^+_c \tau\nu_\tau$ and other heavier states with lower mean $K$-factor. To estimate the positive variation of the $K$-factor distribution the $\Lambda^+_c D^{(*)-}_s$ contribution was reduced to zero, with the $\Sigma_c\pi\mu\nu_\mu$ contribution decreased by 50%. The largest shift in the fitted lifetime was 8.9 $\mu m$ so this is taken as the systematic error due to the branching fractions in the $K$-factor.

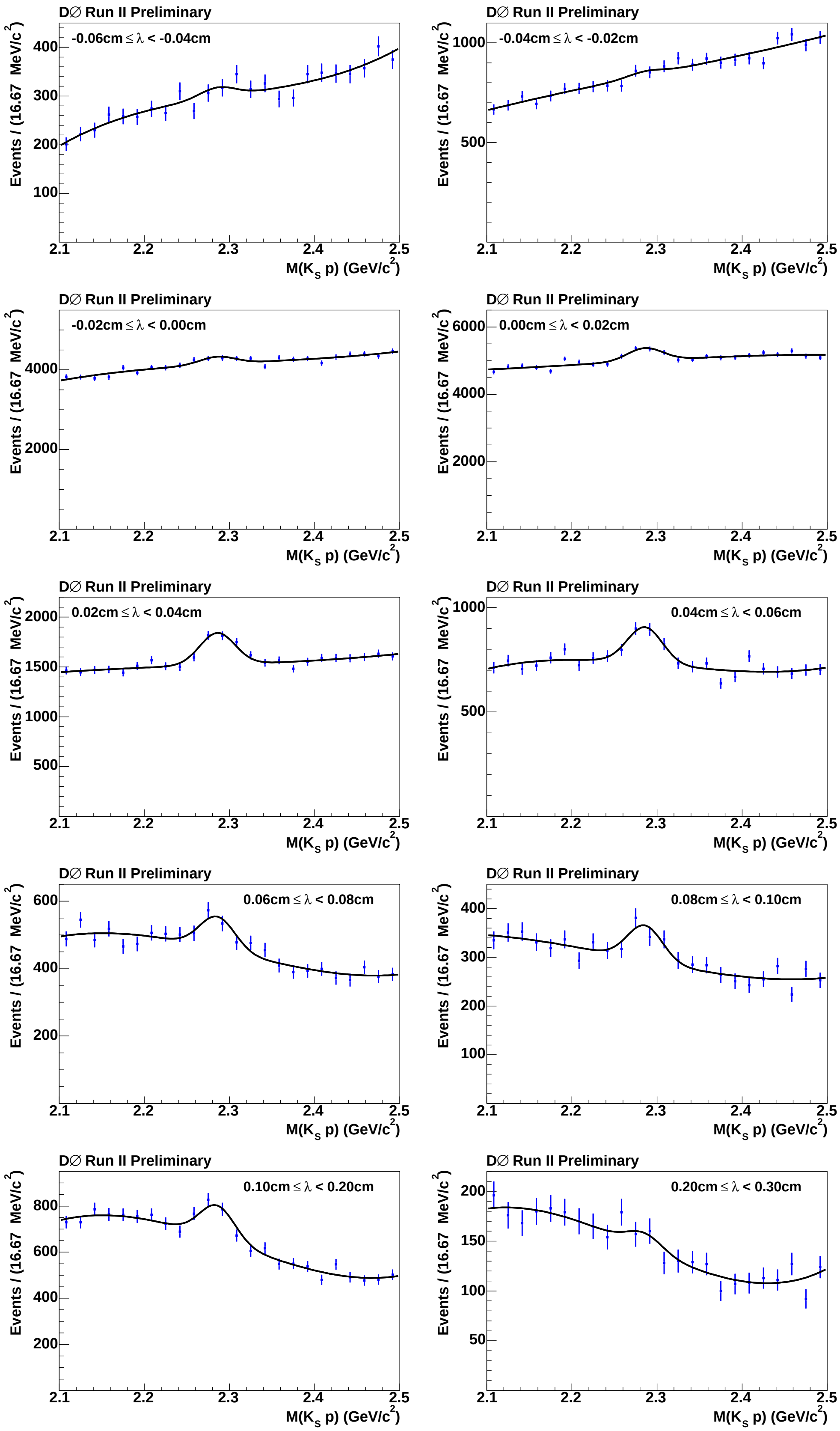


FIG. 4: The mass fits for each of the VPDL intervals

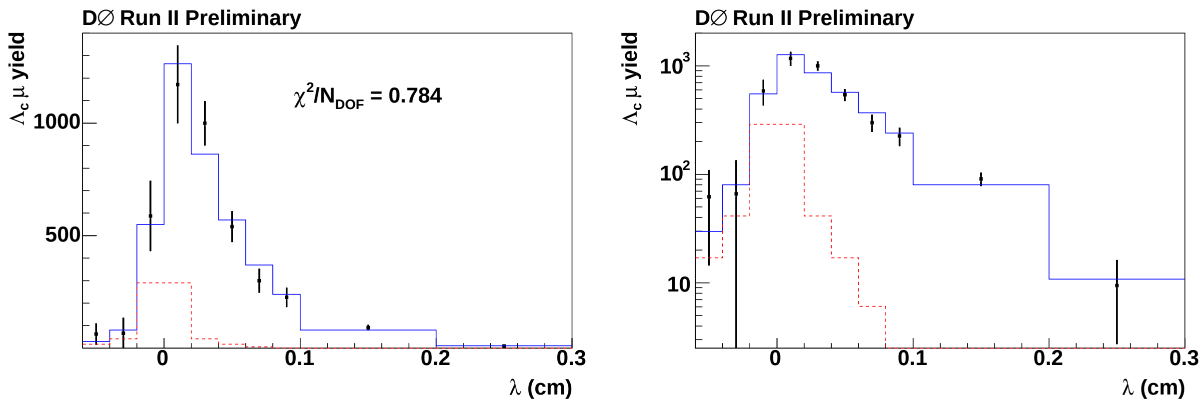


FIG. 5: Measured yields in the VPDL bins and the result of the lifetime fit. The dashed line shows the $c\bar{c}$ contribution. The right plot shows the same distribution in logarithmic scale.

The mean of the $K$-factor distribution does not change significantly with $p_T(\mu)$, however the shape of the distribution is changed. To estimate the effect of this the distribution for $\Lambda_c^+\mu\nu_\mu$ decays was generated with a cut of $p_T(\mu) > 6$ GeV/$c$. The fit was then performed using the distribution with and without the cut. A shift of 1.6 $\mu m$ was observed, so we assume this is the uncertainty due to the momentum dependence of the $K$-factor, and it is added in quadrature with that from the branching fraction estimates.

The change in the $K$-factor distribution due to the uncertainty in generation and decay of $B$ hadrons has been estimated in other analyses to be less than 2% [5]. Therefore we shift all $K$-factor values by $\pm 2\%$, and observe the shift in the fitted lifetime. The largest shift of 7.7$\mu$m is also added in quadrature to the other $K$-factor systematics.

The effect on lifetime measurement of a tracking alignment has been estimated in the lifetime measurement of $\Lambda_b^0$ in the decay $\Lambda_b^0 \to J/\psi\Lambda^0$ [6]. In this analysis shifts of $\pm$ 5.4 $\mu m$ were observed due to the alignment. We quote this as an estimate of the systematic error due to alignment in this analysis.

The systematic errors are summarized and added in quadrature in Table III. In total the systematic uncertainty of this measurement was estimated to be 26.1 $\mu$m.

In addition, a number of consistency checks of this analysis was performed. The fitting procedure was repeated with the simulated $\Lambda_b^0 \to \mu\nu\Lambda_c^+$ events which passed the full reconstruction chain and all selection criteria used in data. The fit gave a value of $c\tau = 369.3 \pm 5.5$ $\mu m$, which is consistent with the generated value of 368 $\mu m$. In this fit the scale factor was released and the fit gave a value of $0.976 \pm 0.054$. The simulated events were also used to test that the reconstructed VPDL is not biased with respect to the generated decay length and that the applied selections have the same efficiency for different values of $\Lambda_b^0$ lifetime.

To test whether any bias is introduced into the result by the fitting procedure 500 toy Monte Carlo samples were produced. In each sample 400 proper decay length values were randomly generated, with signal events being generated with a probability of 0.85, and the remaining events generated as $c\bar{c}$ with a visible proper decay length distribution the same as used in the fit. For the signal events, the lifetime was generated from an exponential distribution, using a mean of 385 $\mu m$. For each event a random $K$-factor value was generated, using the $K$-factor distribution as shown in Fig. 2, and applied to obtain the VPDL. Similarly a VPDL uncertainty was generated using the distribution obtained in data, and the VPDL was randomly smeared by Gaussian distribution according to this uncertainty. For each generated sample the fitting procedure used in data was repeated. This test confirmed that there is no statistically significant bias in the fitted value of lifetime and that the assigned uncertainty is correct.

Another test of this analysis consisted in splitting the data sample into two roughly equal parts using various criteria and measuring the $\Lambda_b^0$ lifetime in each sample independently. The sample was split according to the muon charge, its direction or the chronological date of data taking. All such tests give statistically consistent values of $\Lambda_b^0$ lifetime.

## VII. CONCLUSIONS

Our measurement of the $\Lambda_b^0$ lifetime has given the following preliminary result:

| Source | Systematic uncertainty in $c\tau(\mu m)$ |
|---|---|
| Detector alignment | $\pm 5.4$ |
| Mass fitting method | $\pm 20$ |
| K Factor determination | $\pm 12$ |
| $c\bar{c}$ background | $\pm 2.6$ |
| Scale factor | $\pm 10$ |
| Total | $\pm 26.1$ |

TABLE III: Summary of systematic uncertainties

$$c\tau(\Lambda_b^0) = 384.3^{+35.4}_{-32.8}\ (\text{stat}) \pm 26.1\ (\text{syst})\mu\text{m}; \tag{12}$$

$$\tau(\Lambda_b^0) = 1.28^{+0.12}_{-0.11}\ (\text{stat}) \pm 0.09\ (\text{syst})\ \text{ps}. \tag{13}$$

This result is consistent with our other result on $\Lambda_b^0$ lifetime measured in exclusive decay $\Lambda_b^0 \to J/\psi\Lambda^0$ [6] and with the current world average measurement of $c\tau(\Lambda_b^0) = 1.230 \pm 0.074$ ps [4]. It is very competitive compared to previous measurements.


[1] DELPHI Collab., Eur.Phys.J. **C32** (2004) 185.
[2] S.Catani, Yu.L.Dokshitzer, M.Olsson, G.Turnock, B.R.Webber, Phys.Lett. **B269** (1991) 432 .
[3] V. Abazov *et al.* (DØ Collaboration) , Nucl. Instrum Methods Phys. Res. A **565**, 463 (2006).
[4] W.-M. Yao *et al.* (Particle Data Group), J. Phys. G **33**, 1 (2006).
[5] V. Abazov *et al.* (DØ Collaboration), Phys. Rev. Lett. **94**, 182001 (2005).
[6] V. Abazov *et al.* (DØ Collaboration), Phys. Rev. Lett. **94** 102001 (2005).